# OMNI-DIRECTIONAL MOBILITY USING ACTIVE SPLIT OFFSET CASTORS

**Haoyong Yu**[1]
Massachusetts Institute of Technology
Department of Mechanical Engineering
77 Massachusetts Ave, Cambridge, MA 02139
USA, Tel 617-253-5095, Fax 617-258-7881

**Steven Dubowsky**[2]
Massachusetts Institute of Technology
Department of Mechanical Engineering
77 Massachusetts Ave, Cambridge, MA 02139
USA, Tel 617-253-2144, Fax 617-258-7881

**Adam Skwersky**[1]
Massachusetts Institute of Technology
Department of Mechanical Engineering
77 Massachusetts Ave, Cambridge, MA 02139
USA, Tel 617-253-5095, Fax 617-258-7881

## ABSTRACT

A new concept for omni-directional platform and vehicle design using active split offset castors is presented. An active split offset castor (ASOC) unit consists of two coaxial conventional wheels driven independently and connected to the platform chassis by a link. The kinematics and characteristics of the ASOC are analyzed and compared with conventional active castors and steered wheels. The concept of building omni-directional platforms and vehicles using the ASOC is presented and their design and control are discussed. Experimental results from a prototype omni-directional platform are presented, which demonstrate the feasibility of the concept.

## INTRODUCTION

Omni-directional mobile robots or automated vehicles could perform important tasks in environments congested with static and/or dynamic obstacles and narrow aisles, such as those commonly found in nuclear plants, offices, factory workshops and warehouses, eldercare facilities and hospitals (West and Asada, 1997). Current wheeled vehicle designs based on skid steering have limited mobility due to the non-holonomic constraints of their wheels. While they can generally reach any position and orientation in a plane, they may need very complex maneuvers, complicated path planning and control strategies in a constrained environment (Laumond, 1998). Vehicles with omni-directional mobility would be very desirable for such applications. In this paper, the term omni-directional is used to describe the ability of a system to move instantaneously in any direction from any configuration.

A variety of designs of omni-directional or near omni-directional vehicles have been developed. These can be broken into two approaches: special wheel designs and conventional wheel designs. An omni-directional vehicle is usually formed using three or more of such wheels.

Most special wheel designs are based on a concept that achieves traction in one direction and allow passive motion in another. The universal wheel is an example of the special wheel design that has a number of small passive rollers mounted on the periphery of a normal wheel. The axes of the rollers are perpendicular to that of the wheel (Fujisawa et al., 1997, Ferriere and Raucent, 1998). The wheel is driven in a normal fashion, while the rollers allow for a free motion in the perpendicular direction. The Mecanum wheel design is based on similar concept (Muir and Neuman, 1987). It has angled passive rollers around the periphery of the wheel. By controlling the four wheels attached to a platform, omni-directional mobility can be achieved.

Other special wheel designs of note are the orthogonal wheel developed by Killough and Pin (1994) and the ball wheel mechanism developed by West and Asada (1997). In the ball wheel design, power from a motor is transmitted through gears to an the active roller ring and then to the ball via friction between the rollers and the ball, see Figure 1.

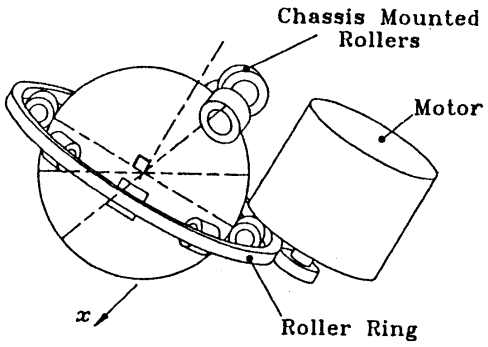


**Figure 1. Ball Wheel Design (West and Asada, 1997)**

Such designs demonstrated good omni-directional mobility, especially the ball wheel design, but they generally have complex mechanical structures. Further, vehicles based on these designs can have limited load capacity when the loads are supported by the slender rollers, such as in the case of universal wheel design. For these designs, the height of obstacles, such as cables on the floor or small steps that they can pass over, is limited by the small diameter of the rollers. Designs with passive rollers also can generate unwanted vibrations as the rollers make successive contact with the ground.

[1] ASME Student Member
[2] ASME Fellow

Conventional wheels are inherently simple, have high load capacity and high tolerance to floor irregularities such as bumps, cracks, dirt and debris. However, due to their non-holonomic nature, they are not omni-directional. Designs have been proposed to achieve near omni-directional mobility for vehicle using conventional wheels. The most common designs are those using steered wheels (Boreinstein, et al., 1996). Vehicles based on this design have at least two active wheels, each of which has both driving and steering actuators. They can move in any direction from any configurations. However, this type of system is not truly omni-directional because it needs to stop and re-orient its wheels to the desired direction whenever it needs to travel in a trajectory with non-continuous curvatures. One technique to use the conventional wheel for omni-directional mobility is to use the active castor wheel, see Figure 2. With two or more such wheels omni-directional mobility can be achieved for a vehicle (Wada and Mori, 1996)

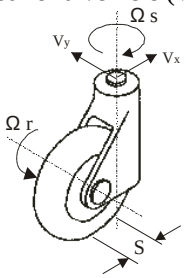


**Figure 2. Active Castor Design**

One major drawback of the above two designs using conventional wheel designs is the high friction and scrubbing during the steering as the wheel is actively twisted around a vertical axis. This reduces positioning accuracy and increases power consumption and tire wear especially for heavy vehicles.

The fundamental cause of the scrubbing problem is that a wheel generates larger frictional forces when steered actively around a vertical axis than when it is rolling. The scrubbing problem can be reduced using the dual wheel design. The duel wheel design is commonly found in the aircraft front landing gear. Wheels in the duel wheel design are always rolling even during steering. The frictional forces they experienced are consistent and substantially smaller than those experienced by the steered wheels and active castors. However, vehicles using dual wheel design are still not omni-directional, as they need to stop and reorient the wheels on some paths.

In this paper, a design called active split offset castor (ASOC) design is presented, see Figure 3. It can achieve omni-directional mobility with reduced wheel scrubbing. A provisional patent application has been file with the US Patent Office. The design is being studied for application to an intelligent walker for elderly people (Dubowsky et al., 2000). It is worth noting that it is necessary to transmit power and signals across the rotary joints for both the conventional active castor design and the ASOC design proposed here. Wada and Mori (1996) used complex gearing system to solve this problem. In the design for the walker for the elderly, slip rings are used at each offset link joint.

In the following sections, the ASOC is analyzed and compared with the conventional active castor wheel. Its design and control issues are discussed along with the experimental results that show its effectiveness.

## ACTIVE SPLIT OFFSET CASTOR AND ITS KINEMATICS

The split offset castor wheel assembly consists of two independently driven coaxial normal wheels, which are separated at a distance D and connected with an offset link of length S to the platform at the joint, as shown in Figure 3.

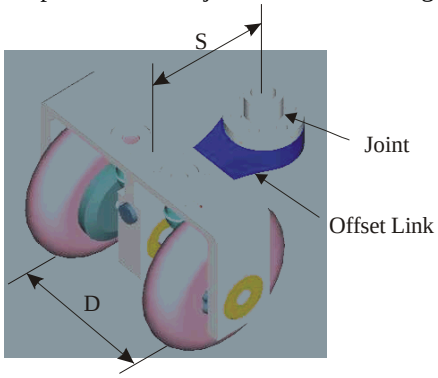


**Figure 3. Split Offset Castor unit**

In the coordinate systems defined in Figure 4, XOY is the inertial coordinate frame and $X_wCY_w$ is the moving coordinate frame attached to the wheel assembly at the offset link joint.

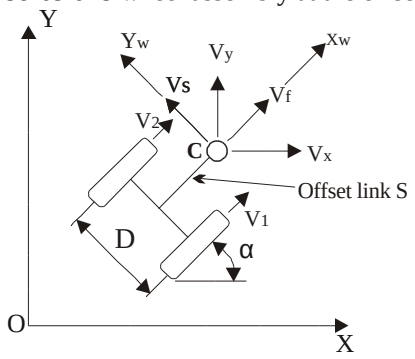


**Figure 4. Coordinate System of the Wheel Assembly**

The wheel and joint (point C in figure 4) linear velocities with respect to ground are $V_1$, $V_2$, $V_f$ and $V_s$ respectively. The two vectors **u** and $q_w$ are defined by:

$$\mathbf{u} = \begin{bmatrix} V_1 & V_2 \end{bmatrix}^T$$
$$\mathbf{q}_w = \begin{bmatrix} V_f & V_s \end{bmatrix}^T \quad (1)$$

The vector $q_w$ can be written as:

$$\mathbf{q}_w = J_w u \quad (2)$$

where:

$$\mathbf{J}_w = \begin{matrix} 1/2 & 1/2 \\ S/D & -S/D \end{matrix} \quad (3)$$

The inertial velocity of C is defined as $\mathbf{q}$ and is given by:

$$\mathbf{q} = \begin{bmatrix} V_x & Vv \end{bmatrix}^T = \mathbf{R}(\acute{a})\mathbf{q}_w \tag{4}$$

where:

$$\mathbf{R} = \begin{matrix} \cos\alpha & -\sin\alpha \\ \sin\alpha & \cos\alpha \end{matrix} \tag{5}$$

Then the kinematic relationship between the inertial velocity of the offset link joint $\mathbf{q}$ and the wheel velocity $\mathbf{u}$ is simply:

$$\mathbf{q} = \mathbf{R}\mathbf{J}_w\mathbf{u} = \mathbf{J}\mathbf{u} \tag{6}$$

By controlling the velocities of the two wheels, arbitrary and unique velocities at the joint of the link can be achieved. Figure 5 shows the simulation results for a wheel assembly producing a velocity of 0.2m/s in the X direction at the joint of the offset link, showing the path of the wheel assembly and the velocities of the two wheels. In this simulation, the distance between the two wheels is D = 0.12m and the offset is S = 0.06m. It can be seen that the wheels follow a smooth trajectory while point C moves perpendicular to the connecting link. The two wheels move in opposite directions first and then both converge to the same velocity as the joint when they are aligned in the moving direction. Although the wheels themselves can not move perpendicular to their original positions, the joint of the offset link can move in any direction instantaneously for any configuration. This is the fundamental feature of the split offset castor design that enables it to achieve omni-directional mobility.

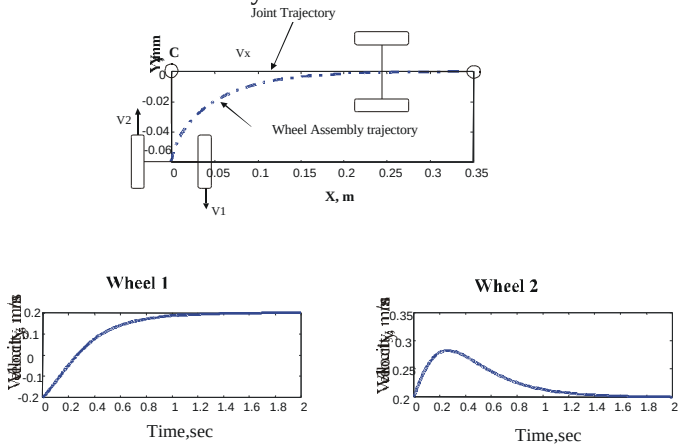


**Figure 5. Simulation of a Split Offset Castor Wheel Assembly**

## OMNI-DIRECTIONAL PLATFORM KINEMATICS

Consider a rigid or vehicle that is carried by ASOC units that move on a plane, then its motion has three degrees of freedom. Then the velocities $x$, $y$ and $\varphi$ can be fully defined by the velocities at the any two distinct points, as shown in Figure 6. If the velocities at these two points can be controlled arbitrarily, omni-directional mobility for the platform is achieved.

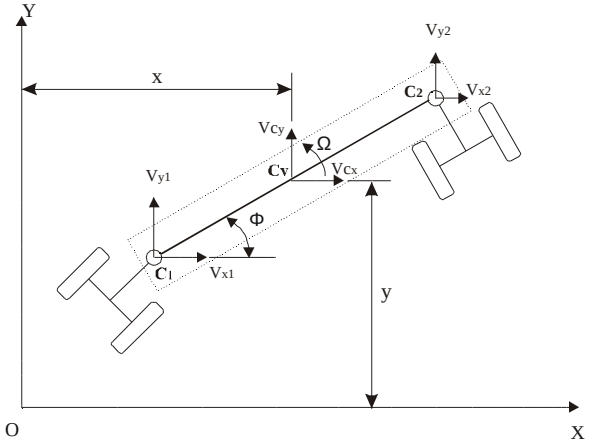


**Figure 6. Platform with two Active Wheel Assemblies**

As shown in the previous section, the ASOC can achieve arbitrary velocity at the joint of the offset link. Thus with a minimum of two ASOC units, an omni-directional mobility platform can be constructed as illustrated in Figure 6. Defining the velocities $V_{cx}$, $V_{cy}$, $\Omega$ at the center of the platform Cv and the velocities $V_{x1}$, $V_{y1}$, $V_{x2}$, $V_{y2}$ of the two joints $C_1$, $C_2$ as:

$$\begin{aligned} \mathbf{p}_v &= \begin{bmatrix} V_{cx} & V_{cy} & \Omega \end{bmatrix}^T \\ \mathbf{q}_v &= \begin{bmatrix} V_{x1} & V_{y1} & V_{x2} & V_{y2} \end{bmatrix}^T \end{aligned} \tag{7}$$

where $\Omega$ is defined as $d\varphi/dt$, the velocities of the platform can be expressed in terms of the velocities at the offset link joints as:

$$\mathbf{p}_v = \mathbf{J}_v\mathbf{q}_v \tag{8}$$

where:

$$\mathbf{J}_v = \begin{matrix} \frac{1}{2} & 0 & \frac{1}{2} & 0 \\ 0 & \frac{1}{2} & 0 & \frac{1}{2} \\ \frac{1}{B}\sin\varphi & -\frac{1}{B}\cos\varphi & -\frac{1}{B}\sin\varphi & \frac{1}{B}\cos\varphi \end{matrix} \tag{9}$$

Given the desired platform velocities, the joint velocities can be obtained with the inverse kinematics expressed as:

$$\mathbf{q}_v = \mathbf{N}_v\mathbf{p}_v \tag{10}$$

where $\mathbf{N}_v$ is a 4x3 matrix given as:

$$\mathbf{N}_v = \begin{matrix} 1 & 0 & \frac{B}{2}\sin\varphi \\ 0 & 1 & -\frac{B}{2}\cos\varphi \\ 1 & 0 & -\frac{B}{2}\sin\varphi \\ 0 & 1 & \frac{B}{2}\cos\varphi \end{matrix} \tag{11}$$

Clearly a vehicle needs a least one additional passive castor wheel for static stability. Additional ASOC units can be used to achieve better traction, but the velocity control must be coordinated to reduce wheel slippage.

## CHARACTERISTICS OF ACTIVE SPLIT OFFSET CASTOR WHEEL DESIGN

The split wheel design has certain advantages over single wheel designs such as the steered wheel and the conventional castor wheel due to the relatively high resistance of twisting a wheel compared to its rolling resistance. A conventional wheel moving on a plane experiences three major resistance forces, as illustrated in Figure 7.

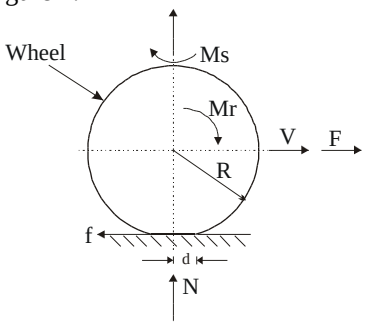


**Figure 7. Resistance Forces on Conventional Wheels**

The first one is the contact frictional force f that prevents slipping. It is related to the normal force N acting on the wheel and the frictional coefficient μ by:

$$f \le \mu N \tag{12}$$

The coefficient of friction, μ, is a characteristic of the wheel and the floor materials. For a rubber wheel and a concrete floor, μ is about 0.8.

The second force, F, is the wheel rolling resistance. F is defined as the force needed to roll the wheel. The coefficient of rolling resistance $\mu_r$ is defined as the ratio of F to the normal force N. $\mu_r$ is in the range of 0.001 to 0.01 depending on the type of wheels and the speed of the wheels (Wong, 1993). For a wheel of diameter R, the rolling resistance moment $M_r$ can thus be expressed as:

$$M_r = \mu_r NR \tag{13}$$

The third resistance force is the scrubbing torque $M_s$. It is the torque required to twist the wheel around its vertical axis. During the steering, a wheel is scrubbing against the floor. This torque is generally high, especially for heavily loaded vehicles. Theoretically, $M_s$ can be calculated by integrating the frictional force elements over the entire contact patch between the wheel and the floor. However this calculation in general is difficult because the shape of the contact patch and the pressure distribution need to determine using the Hertzian contact model that is a function of the load, the compliance and profile of the wheel and floor. Nevertheless, this torque still can be estimated based on some assumptions made about the contacting patch and pressure distribution. For tires with circular profile as shown in Figure 6 (c), the contact patch will be elliptical and for cylindrical tires, the patch will be rectangular, see Figure 6 (d). The pressure distribution will have the form as shown in the Figure (c) and (d).

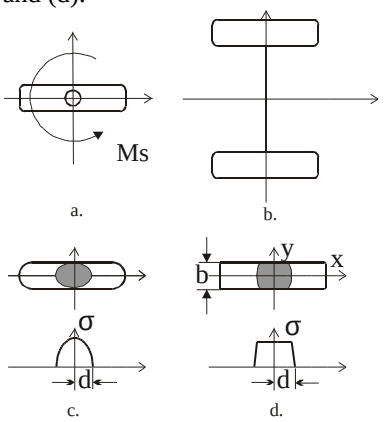


**Figure 8. Comparison between Conventional Castor and Split Offset castor**

Assuming a simple rectangular pressure distribution for the cylindrical tire as shown in Figure 8 (d), the scrubbing torque is estimated as:

$$M_s = \frac{2\beta}{bd} \int_0^d \int_0^{\frac{b}{2}} \sqrt{x^2 + y^2}\, dxdy \tag{14}$$

Where β is a correction factor for the assumption that the pressure is evenly distributed, b is the width of the wheel and d is the width of the contacting patch. If the deformation of wheel radius R is 5%, d will be about 0.3 R.

Taking the robotic walker for the elderly as an example, the radius of the wheel R is 38 mm, the width of the wheel b is 24 mm. Assuming β equal to 0.3, μ is 0.8 and μr is 0.005, for a same normal force N of 100N, the rolling resistance based on Equation (13) is 0.019Nm; the scrubbing torque is 0.215Nm. The scrubbing torque is about 10 times bigger than the rolling resistance.

During the steering, for a steered wheel or a normal castor wheel, the steering actuator needs to overcome the scrubbing torque $M_s$, leading to heavy power consumption and severe tire wear. For the split castor, the resistance moment experienced by the wheel actuators is rolling resistance moment $M_r$ that is much smaller, which results in much less power consumption. Power consumption is one of the key issues for self contained system, such as a robotic walker for the elderly or automatic transport vehicles in factories.

## DESIGN AND CONTROL CONSIDERATIONS

### Selection of Parameters of Wheel Assembly

From the kinematics of the ASOC unit, it can be seen that the velocities of the two wheels depend not only on the velocity at the joint of the offset link but also on platform configurations. The velocities also depend strongly on the ratio between the wheel distance D and the offset S. To illustrate this relationship, a simulation is performed for an ASOC unit with the same D as in the case shown in Figure 4. Here the joint of the offset link moves at 0.3 m/s sideward. Figure 9

shows the simulation results for the velocities of the two wheels for different ratios of S/D.

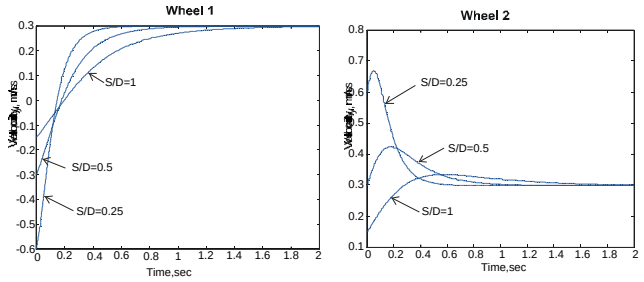


**Figure 9. Effects of S/D on Wheel Velocities**

We can see that the bigger the ratio of S/D, the smaller the velocity change is. Excessive velocity changes can present difficulties for the wheel velocity control and can lead to actuator saturation. Also the needs for rapid change in velocity can lead to wheel slippage. So in general a large ratio of S/D is advantageous. However, large S/D ratios lead to large active split offset castor units. As S/D increases, the footprint of the vehicle will also change as a function of the configuration, leading to size problem and, in some cases, stability problems. For the case of a robotic walker for the elderly, large S/D ratio may make it difficult to move through doorways and between obstacles and can also cause it to interfere with the user's feet. Clearly the selection of S/D for a specific application requires careful trade off design studies.

## Suspension for Mobility Platform

The simplest configuration of a vehicle using this approach will have two ASOC units and one conventional passive castor. This vehicle will have five wheels, all of which must maintain contact with the floor to prevent loss of traction and hence control. For a vehicle, all five wheels would need to be on a same plane and the floor would need to be a perfect plane. In practice, both of these requirements are unobtainable. Although some compliance in the wheel and the mechanical structure will alleviate this problem, it is often not sufficient. To accommodate this problem, some forms of suspension can be built into the systems. For the walker, a simple but effective solution is to add one passive degree of freedom to ASOC unit in the direction perpendicular to the wheel axis, see Figure 10.

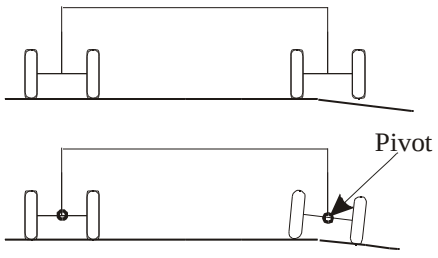


**Figure 10. A Passive Joint Used in Walker Design to Compensate Floor Unevenness**

## Reducing Vehicle Slippage Using Joint Encoders

An omni-directional vehicle has only three degrees of freedom X, Y and φ, See Figure 6. However, with this approach the vehicle need at least two active split offset castor units with at least four actuators. Thus the system is over constrained. This constraint can be modeled by noting that the distance between the two offset link joints must be constant, which results in the following kinematic constraint:

$$V_1 \cos\gamma_1 = V_2 \cos\gamma_2 \qquad (15)$$

Where $\gamma_1$ and $\gamma_2$ are the angles between the line connecting the two joints and the resultant joint velocity $V_1$ and $V_2$ as shown in Figure 11.

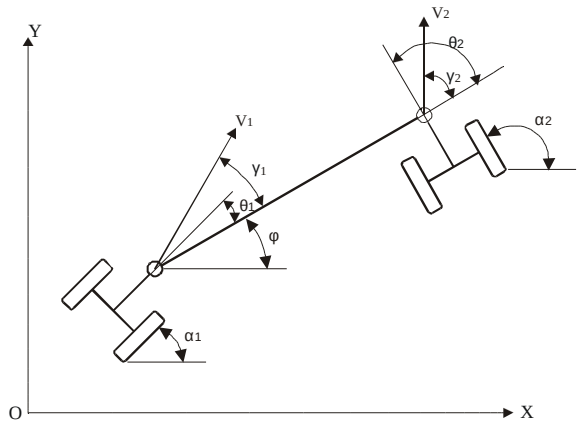


**Figure 11. Kinematic Constraint and Effects of Joint Encoders**

The system controller must ensure that the wheel velocities satisfy this constraint. Violating this constraint will result in wheel slippage and degrade the tracking performance of the system. However, system errors can lead to the violation of kinematic constraints and cause wheel slippage. These errors include mechanical inaccuracy, such as errors in wheel diameter, parameters S, D and B. These structural errors can be effectively eliminated through measurement and calibration. Wheel and structure deformation under various loading conditions and variations of floor condition, such as debris, bumps, cracks and slippery areas on the floor, will degrade the system accuracy. Finally, wheel velocity control also has errors due to limited bandwidth and saturation. In practice many of these error sources are unavoidable. In this study, design and control methods to deal with the slippage and improve the system performance were investigated.

First the individual angles between the platform chassis and each offset link are measured using encoders to ensure that the wheel velocity commands satisfy the kinematic constraint expressed with Equation (14).

Referring to Figure 6, to have the platform follow a desired velocity ($V_{cx}$, $V_{cy}$, Ω), the inverse kinematic Equations (10) and (11) are first solved to yield the joint velocities of the wheel assemblies ($V_{x1}$, $V_{y1}$, $V_{x2}$, $V_{y2}$) as a function of the platform orientation φ. Then using these joint velocities, the wheel velocities are obtained using Equations (1) to (6). Both the

orientation of the ASOC units, $\alpha_1$, $\alpha_2$ and the orientation of the platform, $\varphi$, must be known in order to solve the equations. Any errors in $\alpha_1$, $\alpha_2$, $\varphi$ and the wheel velocities will degrade the inverse kinematics process.

The values of $\alpha_1$ and $\alpha_2$ for the ASOC units can be obtained via dead reckoning based on the wheel encoder signal and then $\varphi$ calculated. However this is not reliable because of wheel slippage. The method used here to obtain the absolute position and orientation information of the platform is to use a vision-based localization system, which is described in the next section. In fact, such a sensor system is part of the walker system and is used for navigation and localization [9]. While this sensor system provides a good knowledge of $\varphi$, it can not provide the $\alpha$'s for wheel assemblies. These values are obtained using the encoders on the offset link joints. In the case of manual control, it is not necessary to know the absolute orientation of the platform. The joint encoders are sufficient to ensure smooth motion of the platform.

## TEST-BED PROTOTYPE AND EXPERIMENTAL RESULTS

To demonstrate the omni-directional mobility design concept and evaluate its performance, an experimental test-bed has been built, as shown in Figure 12.

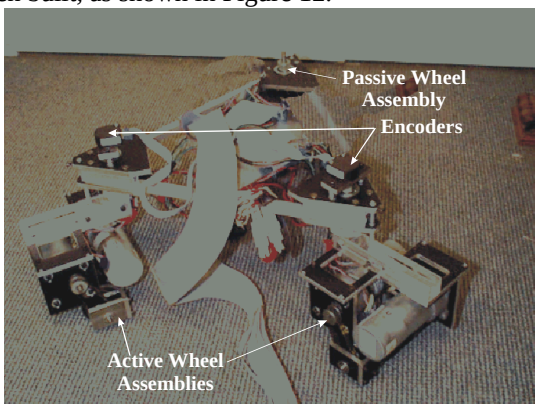


**Figure 12. Test Bed Platform**

The experimental system has two ASOC units and one passive split offset castor unit. Each active unit is driven by a gear-head DC motor with an optical encoder. Each offset link joint has an optical encoder.

The control system is implemented using a PC equipped with D/A and encoder interface boards and a power amplifier. The platform can be can be controlled manually using velocity commands or operate in an autonomous mode using preplanned trajectories.

The autonomous trajectory tracking implements close-loop control using the absolute position and orientation information of the platform in the inertial coordinate as feedback. The information is obtained using a vision based localization system. The system uses a CCD camera mounted on the platform looking up at encoded signposts on the laboratory ceiling. Each signpost has three elements, an orientation marker, a centerpiece marker an identification marker, see Figure 13. The localization system continually determines the position and orientation of the platform in the inertial coordinate. The vision localization calculation is done on a second PC, which communicates with the control PC via wireless modem as shown in Figure 14. Figure 15 shows the block diagram of the control of the experimental system.

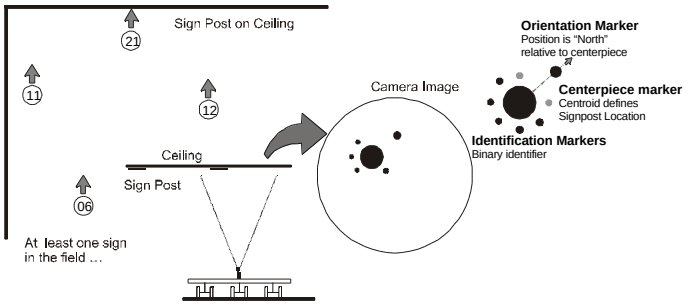


**Figure 13. Vision-Based Localization Method.**

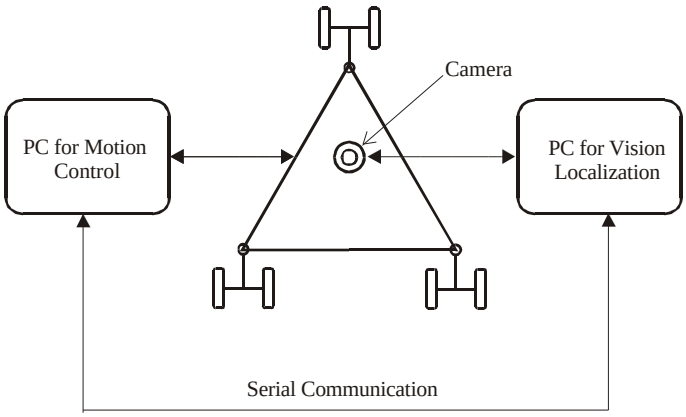


**Figure 14. Experimental Set-up**

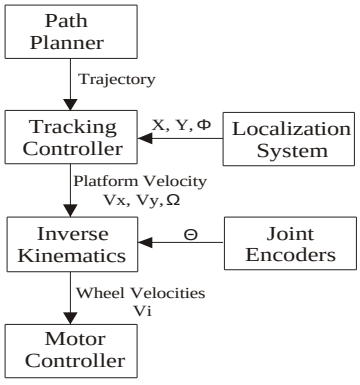


**Figure 15. Experimental System Control Diagram**

To demonstrate the omni-directional mobility, a number of experiments were performed, including circular motions, rectangular motion, and combined translational and rotational motions. The test-bed demonstrated smooth motion even for

complex trajectories. As expected, there are tracking errors for complex trajectories under open loop control, but the system achieved very good tracking accuracy under close-loop. Figure 16 shows a tracking result for a square trajectory of 1.2 m by 1.2 m at a constant speed of 0.05m/s. The system does not stop at the corners of the target. Figure 16 (a) shows that there are substantial errors with dead reckoning under open loop control. The error is about 35 cm at the end of the trajectory. Figure 16 (b) shows that with close-loop, the maximum error along the trajectory is reduced to less than 6 cm.

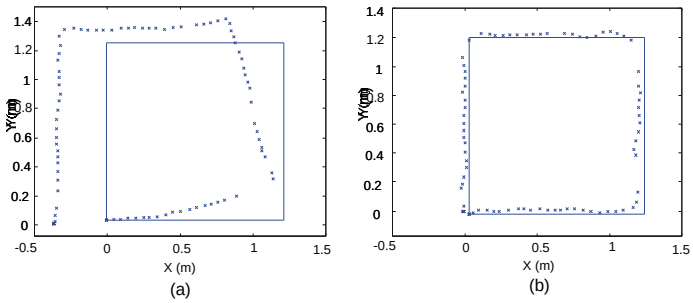


**Figure 16. Square Trajectory Tracking**

## CONCLUSIONS

In this paper, a new concept for omni-directional mobility platform design is presented. It is based on the active split offset castor design. Each active split offset castor unit has two coaxial and independently driven wheels that are connected to the platform via an offset link. An omni-directional platform can be constructed with a minimum of two active split offset castor units and one passive castor. The design offers some advantages over existing omni-directional platforms based on special wheel designs. These advantages include simple mechanical structure, high loading capacity, vibration free and smooth motion and robustness to floor conditions. It has significantly lower wheel scrubbing than conventional the active castor designs. It is thus more power efficient. The concept has been experimentally tested with a test-bed platform. The results demonstrate its omni-directional mobility and the ability to be controlled by a vision based localization system. The concept is being used as the mobility platform for an intelligent omni-directional walker for elderly.

## ACKNOWLEDGMENTS

This work is sponsored by the Home Automation and Health Care Consortium in the MIT d'Arbeloff Laboratory for Information for Information. The efforts of Lani Rapp and Daniel Santos for designing and building the test-bed are appreciated.

## REFERENCES

Boreinstein , J., Everett, H.R. and Feng, L., 1996, *Navigating Mobile Robot*. AK Peters, Wellesley, Massachusetts.

Dubowsky, S., Genot, F., Godding, S., Kozono. H, Skwersky, A., Yu, H., and Yu, L, 2000, "PAMM - A Robotic Aid to the Elderly for Mobility Assistance and Monitoring: A Helping-Hand for the Elderly". *IEEE International Conference on Robotics and Automation*, Accepted

Ferriere, L., and Raucent, B., 1998, "ROLLMOBS, a New Universal Wheel Concept", Proceedings o*f IEEE International Conference on Robotics and Automation*, Leuven, Belgium, pp.1877-1882.

Fujisawa, S., Ohkubo, K., Yoshida, T., Satonaka, N., Shidama, Y., and Yamaura, 1997, H., "Improved Moving Properties of An Omnidirectional Vehicle Using Stepping Motor", *Proceedings of the 36th Conference on Decision & Control*. San Diego, California, pp.3654-3657.

Killough, S.M., and Pin, F.G., 1994, "A New Family of Omnidirectional and Holonomic wheeled platforms for mobile robots", *IEEE Transactions on Robotics and Automation*, Vol.10, No.4, pp. 480-489.

Laumond, J.P., 1998, *Robot Motion Planning and Control*. Springer-Verlag, London.

Muir, P.F., and Neuman, C.P., 1987, "Kinematic Modeling for Feedback Control of an Omni-directional Wheeled Mobile Robot", Proceedings of *IEEE International Conference on Robotics and Automation*, pp. 1772-1778.

Wada, M., and Mori, S, 1996, "Holonomic and Omnidirectional Vehicle with Conventional Tires", Proceedings of *IEEE International Conference on Robotics and Automation*. Minnesota, pp. 3671-3676.

West, M., and Asada, H., 1997, "Design of Ball wheel Mechanisms for Omnidirectional Vehicles With Full Mobility and Invariant Kinematics", *Journal of Mechanical Design*, Vol.119, pp153-161.

Wong, J. Y., 1993 *Theory of Ground Vehicles*. Second edition. Wiley Interscience.